

Three-dimensional warm plasma simulations for low-frequency waves

N. Mellet*, P. Popovich[†], W.A. Cooper*, L. Villard* and S. Brunner*

*Ecole Polytechnique Fédérale de Lausanne, Centre de Recherches en Physique des Plasmas, Association Euratom-Confédération Suisse, CH-1015 Lausanne, Switzerland

[†]Currently at Center for Multi-Scale Plasma Dynamics, Dept. of Physics and Astronomy, UCLA CA 90095-01547 Los Angeles, USA

Abstract. A full-wave code [1, 2] for the wave propagation studies in the Alfvén and the ion-cyclotron frequency domain in 3D plasmas is presented. Two models are implemented: the cold and the warm one where kinetic effects are taken into account in the limit of small Larmor radius. Due to the Fourier discretization in the poloidal and the toroidal directions the parallel wave vector expression is relatively simple. However, the exact computation of k_{\parallel} in 2D and 3D configurations is complicated because of the dependence on both the spatial position and the (m, n) mode numbers considered. A comparison with a 2D PENN [8] code is presented, where we use different approximations for the value of the parallel wave vector. Parallelisation and optimisation of the cold plasma version of the LEMan code is also discussed. Due to improved matrix construction and storage algorithms, the memory requirements are considerably reduced, which allows for calculations in the IC frequency range in the stellarator geometry.

Keywords: Plasma waves, low-frequency, Alfvén, ion-cyclotron, warm model, 3D

PACS: 52.35.-g, 52.35.Bj, 52.35.Hr

INTRODUCTION

Low-frequency waves have an important role to play in fusion. On the one hand, the ion-cyclotron resonance heating (ICRH) is used in devices like JET or LHD and is also planned in ITER. On the other hand, the global modes that take place in the Alfvén domain are of fundamental interest because of their interaction with fast ions. Due to increasing available computational resources, full-wave simulations required at low frequencies are now possible for 2D and 3D configurations [3, 4, 5, 6, 7].

FORMULATION

A full wave treatment is required here because of the strong variation of the space-dependent parameters over one wavelength at low frequencies. The code solves the Maxwell's equations expressed in terms of the electromagnetic potentials (A, ϕ) in order to avoid the numerical pollution:

$$\begin{cases} \vec{B} = \nabla \times \vec{A} \\ \vec{E} = -\nabla\phi + ik_0\vec{A} \end{cases} \Rightarrow \begin{cases} \nabla^2\vec{A} + k_0^2\hat{\epsilon} \cdot \vec{A} + ik_0\hat{\epsilon} \cdot \nabla\phi = -\frac{4\pi}{c}\vec{J}_{ext} \\ \nabla \cdot (\hat{\epsilon} \cdot \nabla\phi) - ik_0\nabla \cdot (\hat{\epsilon} \cdot \vec{A}) = -4\pi\rho_{ext} \end{cases} \quad (1)$$

where the Coulomb gauge is used in the potential formulation. This set of equations is solved using the Galerkin method, multiplying the equations by test functions and integrating over the volume considered, thus removing the second derivatives. Radial finite elements (linear or cubic) and Fourier harmonics in the toroidal and poloidal directions are used for the representation of the solution. This provides a linear set of equations where the matrix of the coefficients has a block-tridiagonal shape. The right-hand side is defined by the antenna currents. More details about the numerical formulation are presented in Ref.[1].

WARM AND COLD MODEL

The cold model has the advantage to be the simplest case and to be able to modelise global Alfvén eigenmodes as well as mode conversion to the Surface Quasi-Electrostatic Wave (SQEW) at Alfvén resonances. However, it can not describe the Kinetic Alfvén Wave, that is more relevant for core fusion plasma. The SQEW exists only at the border of the plasma where the temperature is sufficiently low. To obtain the KAW branch, finite temperature effects have to be taken into account. We have thus implemented a warm model that incorporates the parallel electron Landau damping (instead of the artificial damping parameter in the cold version) and can describe the mode conversion to the KAW.

Both the cold and the warm model formulations satisfy the equation (1), the only difference residing in the dielectric tensor $\hat{\epsilon}$. The dielectric tensor relates the plasma current and the electric field. In the cold model, it is derived using the equation of motion of the charged particles. An artificial "friction force" is added to provide a damping mechanism, which results in a small imaginary part in the frequency ω^* :

$$\begin{aligned} \epsilon_{nn} = \epsilon_{bb} &= 1 - \sum_k \frac{\Pi_k^2}{\omega/\omega^*(\omega_k^{*2} - \Omega_k^2)} & \epsilon_{bn} = \epsilon_{nb} &= 1 - \sum_k \frac{\Omega_k}{\omega} \frac{\Pi_k^2}{\omega_k^{*2} - \Omega_k^2} \\ \epsilon_{\parallel\parallel} &= 1 - \sum_k \frac{\Pi_k^2}{\omega\omega_k^*} & \epsilon_{n\parallel} = \epsilon_{\parallel n} = \epsilon_{b\parallel} = \epsilon_{\parallel b} &= 0 \end{aligned} \quad (2)$$

where Ω_k corresponds to the cyclotron and Π_k to the plasma frequency of the species considered.

The warm plasma model of LEMan is derived from the Vlasov equation:

$$\frac{\partial f}{\partial t} + \vec{v} \cdot \frac{\partial f}{\partial \vec{x}} + \frac{q}{m} [\vec{E} + \vec{v} \times \vec{B}] \cdot \frac{\partial f}{\partial \vec{v}} = 0. \quad (3)$$

Keeping only 0^{th} order Larmor radius terms, the following relation is obtained after linearization:

$$[-i\omega + v_{\parallel} \nabla_{\parallel} + i\Omega] f_1 = -\frac{q}{m} \vec{E}_1 \cdot \frac{\partial f_0}{\partial \vec{v}} = A(\vec{E}, \vec{v}), \quad (4)$$

where f_0 is considered to be a Maxwellian and a Fourier transform in time has been performed for f_1 and E_1 .

Due to the Fourier representation in the poloidal and toroidal directions in LEMan, the parallel wave vector takes a simple form:

$$k_{\parallel} = -i\nabla_{\parallel} = -\frac{i}{\sqrt{g}B} \left(\psi' \frac{\partial}{\partial \theta} + \phi' \frac{\partial}{\partial \varphi} \right) = \frac{1}{\sqrt{g}B} (\psi' m + \phi' n). \quad (5)$$

This expression involves not only the perturbation mode numbers (m, n) , but also the real-space dependent quantities, which complicates the calculations. In the present work, an approximate expression for the wave vector is used [9]. In axisymmetric geometry, a Fourier transform of the Vlasov equation in the toroidal angle can be performed. In this case, the approximation used for the parallel wave vector may not depend on both the poloidal mode and poloidal coordinate. Following this procedure, the dielectric tensor elements are the same as in a cylindrical geometry:

$$\begin{aligned} \varepsilon_{nm} = \varepsilon_{bb} &= 1 - \frac{1}{2\omega} (\tilde{Z}_1 + \tilde{Z}_{-1}) & \varepsilon_{nb} = -\varepsilon_{bn} &= -\frac{i}{2\omega} (\tilde{Z}_1 - \tilde{Z}_{-1}) \\ \varepsilon_{\parallel\parallel} &= 1 + \frac{2}{(k_{\parallel} v_{th})^2} (\omega_p^2 - \omega \tilde{Z}_0) & \varepsilon_{n\parallel} = \varepsilon_{\parallel n} = \varepsilon_{b\parallel} = \varepsilon_{\parallel b} &= 0 \end{aligned} \quad (6)$$

$$\tilde{Z}_l = \frac{\omega_p^2}{\omega - l\Omega} Z^{Sh}(z_l) \quad \text{with} \quad z_l = \frac{\omega - l\Omega}{|k_{\parallel}| v_{th}}, \quad Z^{Sh}(z) = \frac{z}{\sqrt{\pi}} \int_{-\infty}^{\infty} \frac{1}{z-x} e^{-x^2} dx.$$

BENCHMARK AGAINST PENN

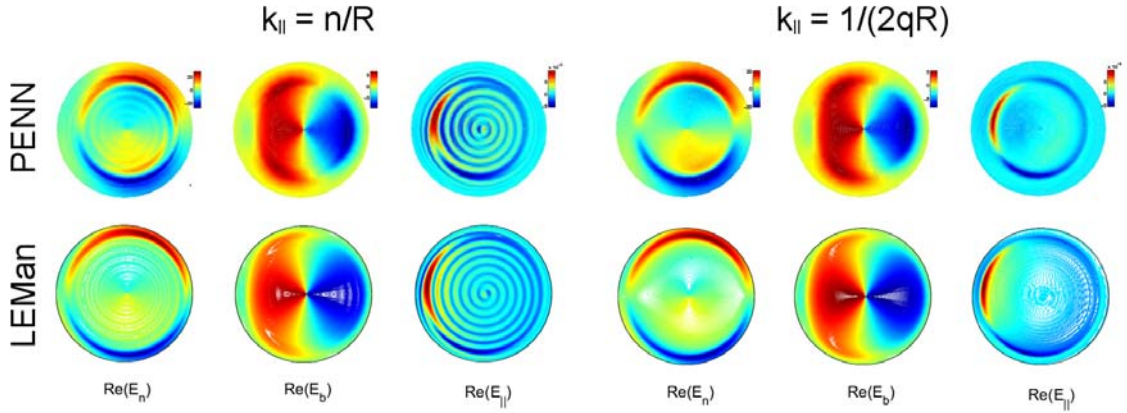


FIGURE 1. Comparison of the wavefields obtained with PENN and LEMan in the case of a mode conversion at the Alfvén resonance for two different approximations for the parallel wave vector.

The plasma model of the full-wave 2D PENN code describes the FLR effects to the 2nd order. For the comparison with the LEMan results, we use the reduced version that only includes the 0th order effects. In Figure 1, a comparison of the results obtained with the two codes is presented for the case of the mode conversion to the KAW at the Alfvén resonance.

The results are almost identical for both codes, the discrepancy coming essentially from a different implementation of the vacuum region between the plasma and the

conducting shell. We can see also the difference between the two approximations for the parallel wave vector which points out the importance of an adequate computation of this term.

PARALLELIZATION

Two different methods are presented here to improve performance using parallelization. Each of them has its own domain of application.

The idea of the first method is to permit computation of cases with spatially localised antenna. In a tokamak, for example, the computation of a high-field or low-field side antenna was possible considering only one toroidal Fourier mode n . For a toroidally localised antenna, several toroidal modes are excited simultaneously. The method takes advantage of the fact that there is no coupling between modes with different n in an axisymmetric configuration. The computation can be, in that sense, totally independent for each n considered, what leads to a perfect parallelization because the CPU time and memory are just divided by the number of processors.

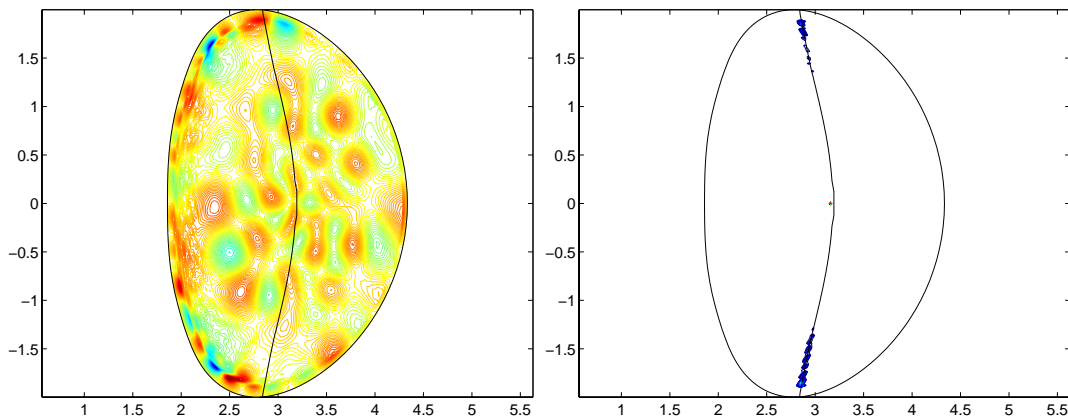


FIGURE 2. Binormal component of the electric field (left) and power deposition (right) for a JET equilibrium. The vertical line corresponds to the deuterium cyclotron resonance. The antenna is localised in the toroidal direction

In figure 2, a case computed with this method is shown. A wave in the IC frequency range is launched from a high-field side antenna in a JET equilibrium configuration. The warm model is used here with the approximation $k_{\parallel} = n/R$ for a deuterium plasma at 3keV. The absorption occurs close to the cyclotron resonance. This is to be expected since in the warm model in the IC domain, the dielectric tensor has an imaginary part only close to this region. 25 different toroidal and 51 poloidal Fourier modes have been used for the computation which gives a total of 1275 (m,n) couples. The antenna occupies the third of the toroidal extension which leads to a dominant excitation of the $n = 3$ Fourier harmonic.

In order to simulate ion cyclotron waves in stellarators, another method has been developed to optimize the parallel solver of the LEMan code. The problem comes from the fact that in this range of frequencies, the number of Fourier harmonics required considerably increases due to the smaller wavelengths and to the fact that the resonant

surfaces cross the magnetic surfaces. The memory required for the matrix storage scales as a square of the total number of the harmonics. The total memory becomes the critical parameter to be reduced via the parallelization.

The magnetic surfaces are distributed here over the processors instead of the different toroidal mode numbers as before. The matrix has a block-tridiagonal shape, each block is dense because of the coupling between the Fourier modes. It is unfortunately too broad to be solved by SCALAPACK using the band representation due to the huge size of temporary arrays in this case. Thus, the method used here is BABE [10] (Burn At Both Ends), which consists of a Gauss decomposition beginning from the top and from the bottom of the matrix at the same time. Eventhough it is a "2 processors" method, it has the advantage to be more efficient in time than cyclic reduction with less than 32 processors. It can also be well optimised for data storage and some possibilities still exist to improve its speed.

An optimization of the memory usage is done by performing the Gauss decomposition at the same time as the matrix construction. This allows to store only one block for each magnetic surface instead of three with the previous method. The first one is eliminated by the Gauss decomposition itself, while the second is removed by performing a multiplication that is normally carried out during the backsolve.

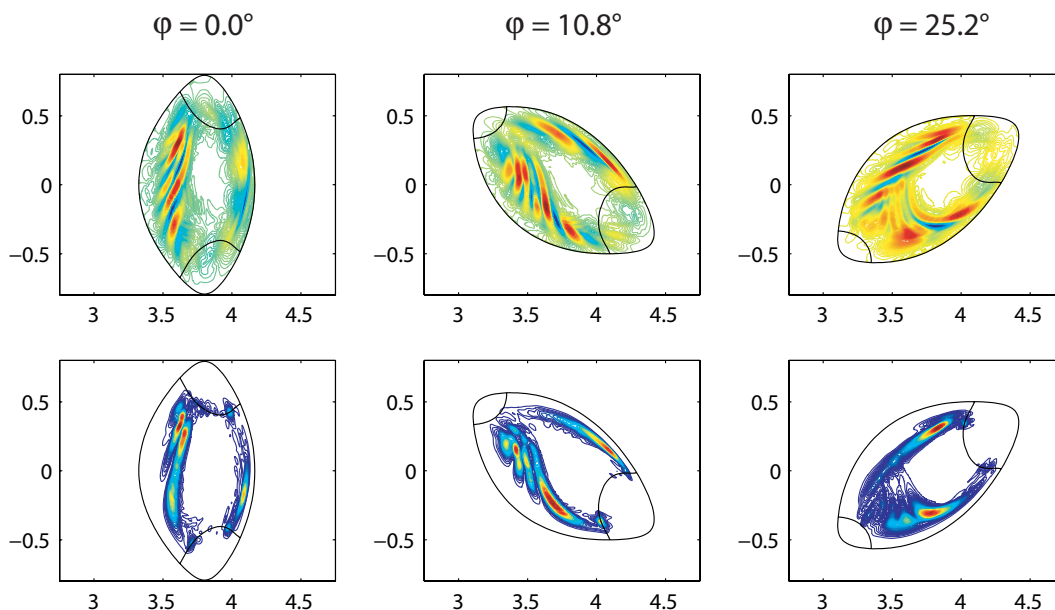


FIGURE 3. Normal component of the electric field (top) and power deposition (bottom) for the LHD stellarator. The lines correspond to the deuterium cyclotron resonance.

Finally, the CPU time can also be reduced. Several operations inside the Gauss decomposition such as a matrix multiplication can be parallelized by distributing a part of the columns over the processors.

All of these improvements permit now the computation of cases that requires a huge amount of memory such as the LHD case presented above. The simulation was made on the Pleiades 2 cluster in EPFL on 48 pentium 4 processors (2.8 GHz, 4 GB each). This calculation is performed with 200 radial elements and 630 Fourier harmonics which

would have corresponded to 490 GB in a LAPACK band representation for the matrix to be solved.

The simulation shows the deuterium plasma response to an excitation in the IC domain. The cold plasma model is used for this computation. The power deposition occurs close to the resonant surfaces (where the deuterium cyclotron frequency corresponds to the frequency of the injected wave) and where the cyclotron wave can propagate.

CONCLUSION

The new optimisation of the LEMan code allows now the computation of stellarator configurations in the ICRF domain using the cold plasma model. An example is presented for a configuration of the LHD stellarator for which the zones of absorption coincide with the resonant surfaces and where the ion-cyclotron wave can propagate.

For the warm plasma model, comparisons have been made with the PENN code using approximated values for the parallel wave vector. The results are in a good agreement but point out the importance of an exact computation of k_{\parallel} . A version incorporating the exact computation of the parallel wave vector is now in development.

ACKNOWLEDGMENTS

We thank Dr. S.P. Hirshman for the use of the VMEC code and are grateful to A. Jaun for the results of the PENN code. This work was partly supported by the Swiss National Science Foundation and Euratom. The major part of the calculations was performed on the Pleiades cluster in EPFL.

REFERENCES

1. P. Popovich, W.A. Cooper, and L. Villard, *Comp. Phys. Comm.*, **175**(4), 250 (2006).
2. P. Popovich, W.A. Cooper, and L. Villard, *Fus. Sci. & Tech.* **46**(2), 342 (2004).
3. E. F. Jaeger, L. A. Berry, E. D'Azevedo, D. B. Batchelor, M. D. Carter, K. F. White, and H. Weitzner, *Phys. Plasmas*, **9**(5), 1873 (2002).
4. A. Fukuyama, T. Akutsu, *43rd Annual Meeting of the APS Division of Plasma Physics, Long Beach, California, Oct. 29 - Nov. 2, 2001*.
5. M. Brambilla, *Phys. Control. Fusion*, **41**(1), 1 (1999)
6. E.A. Lerche, and P.U. Lamalle, *Theory of Fusion Plasmas, Joint Varenna-Lausanne International Workshop 2004*, p.359.
7. L. Villard, K. Appert, R. Gruber, and J. Vaclavik, *Comput. Phys. Reports*, **4**, 95 (1986).
8. A. Jaun, A. Fasoli, D. Testa, J. Vaclavik, and L. Villard, *Plasma Phys. Control. Fusion*, **43**, A207 (2001).
9. S. Brunner, and J. Vaclavik, *Phys. Fluids B* **5**, 1695 (1993).
10. R. Gruber, W.A. Cooper, M. Beniston, M. Gengler, and S. Merazzi, *Physics Reports* **207**, 167 (1991).